

Memory and Kovacs effects in the parking-lot model: an approximate statistical-mechanical treatment

G. Tarjus^a and P. Viot^a

^aLaboratoire de Physique Théorique des Liquides, Université Pierre et Marie Curie, 4, place Jussieu, 75252 Paris Cedex, 05 France

The parking-lot model provides a qualitative description of the main features of the phenomenology of granular compaction. We derive here approximate kinetic equations for this model, equations that are based on a 2-parameter generalization of the statistical-mechanical formalism first proposed by Edwards and coworkers. We show that history-dependent effects, such as memory and Kovacs effects, are captured by this approach.

1. Introduction

The term of “glassy-dynamics” is now commonly used to describe out-of-equilibrium systems that display such generic features as very slow kinetics that prevent the system from reaching equilibrium in any reasonable experimental timescale, aging phenomena, history-dependent processes like hysteresis and memory effects. Among such systems are the “not-too-strongly” vibrated granular materials[1, 2, 3, 4, 5]. In the recent years, there has been a surge of research activity in this field[6, 7, 8], partly driven by the goal of providing a statistical-mechanical description of these out-of-equilibrium situations[9, 10, 11, 12][13, 14, 15, 16, 17, 18, 19].

In this note, we consider an approximate statistical-mechanical description of the parking-lot-model (PLM) for vibrated granular materials[2, 3, 20, 21, 22, 23, 24] that is based on the formalism proposed by Edwards and coworkers[9, 10, 11, 12]. Despite its simplicity, the one-dimensional model of random adsorption-desorption of hard particles (PLM) has the merit of being a microscopic, off-lattice model that mimics many features of the compaction of a vibrated column of grains. It also has, we hope, a didactic value as to the nature of several canonical characteristics of “glassy dynamics”. Many of the properties of the model, that can be obtained either analytically or by computer simulation, have been already described in the literature[2, 3, 20, 21, 22, 23, 24, 25, 26]. Our main focus here is on memory effects, including the so-called Kovacs effect first observed in glassy polymers[27, 28](see also[29, 30, 31, 32]), and on the ingredients that are needed in a statistical-mechanical description to account for such effects.

2. The model and its properties

The parking-lot model is one-dimensional process in which hard rods of length σ are deposited at random positions on a line at rate k_+ and are inserted successfully only

if they do not overlap with previously adsorbed particles; otherwise they are rejected. Moreover, all deposited particles can desorb, i.e., be removed from the line at random with a rate k_- . For convenience, the unit time is set to $1/k_+$, and the unit length to σ . With this choice of units, the only control parameter in the model is $K = k_+/k_-$. When desorption is forbidden ($k_- = 0$), the model corresponds to the purely irreversible one-dimensional random sequential adsorption (RSA) process[33, 34], also known as the car parking problem, and all the properties of the system as a function of time can be obtained exactly. Connection to the compaction of a vibrated column of grains is made by considering the line as average layer (a 2-dimensional model would be more realistic, but the qualitative behavior would not be altered), the time as the number of taps, and $1/K$ as the tapping strength that controls the fraction of particles ejected from the layer at each tap.

When $1/K$ is not strictly equal to zero, adsorption and desorption are competing mechanisms that drive the system to a steady state corresponding to an equilibrium fluid of hard rods at a constant activity $1/K$. All the properties of the steady-state can also be obtained exactly.

The compaction kinetics of the parking-lot model at constant K is described by

$$\frac{\partial \rho}{\partial t} \Big|_K = \Phi(t) - \frac{\rho(t)}{K} \quad (1)$$

where $\rho(t)$ the density of hard rods on the line at time t and $\Phi(t)$ is the fraction of the line that is available at time t for inserting a new particle, i.e., the probability associated with finding an interval free of particles (a “gap”) of length at least 1. The quantities ρ and Φ can be obtained from the 1-gap distribution function $G(h, t)$ which is the density of gaps of length h at time t via a number of “sum rules”:

$$\rho(t) = \int_0^\infty dh G(h, t) = 1 - \int_0^\infty dh h G(h, t), \quad (2)$$

$$\Phi(t) = \int_1^\infty dh (h-1) G(h, t). \quad (3)$$

The 1-gap distribution function $G(h, t)$ obeys a kinetic equation that also involves 2-gap distribution function. Similarly, the kinetic equation of the 2-gap distribution involves the 3-gap distribution function, and so on[25]. The resulting infinite hierarchy of coupled equations cannot in general be solved analytically (exceptions are the RSA, when $k_- = 0$ and equilibrium when $t \rightarrow +\infty$).

The description of the kinetics of the parking lot model at large, constant K (i.e. small, constant tapping strength) can be summarized as follows: the density increases monotonically during the process, and the kinetics can be considered as a succession of four different regimes (see Fig. 1): during a first stage, the density increases rapidly until a value of around 0.65, and it is followed by an algebraic approach toward the saturation density, $\rho_{JL} = 0.747\dots$ of the model without desorption (RSA); around this density there is a crossover to a still slower $1/\ln(t)$ compaction regime that is reminiscent of what is exactly observed when $1/K \rightarrow 0$, and finally there is an exponential approach to the steady-state (equilibrium) density with a rate $\Gamma \sim \frac{(\ln(K))^3}{K^2}$. For the two first

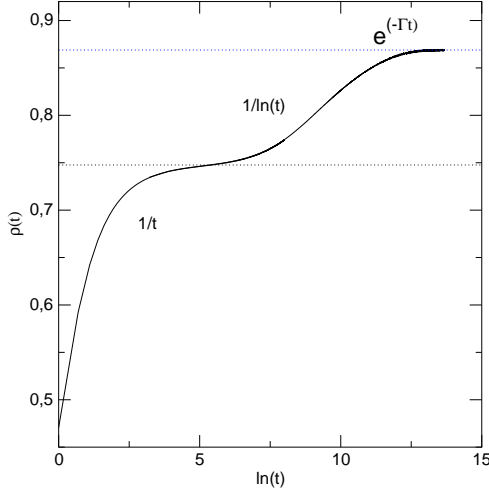


Figure 1. Logarithmic-linear plot of the density versus time for the parking-lot model at a constant tapping strength $1/K = 0.0002$

regimes, desorption has a negligible effect and only the two last regimes are relevant for the compaction kinetics of vibrated granular materials (although the approach to equilibrium may be prohibited when K is very large).

Experimentally, it has been observed that granular compaction exhibits history-dependent phenomena. In particular, Josserand *et. al.*[4] have shown that memory effects are seen when changing the tapping strength during the compaction kinetics. Similar effects have been found in the parking-lot model, when the tapping strength $1/K$ is switched at a given time to a larger (or smaller) value: see Fig. 2

The obvious lesson that one can draw such memory effects is that whereas equilibrium is fully described by one thermodynamic parameter, the density ρ , out-of-equilibrium situations require at least one additional “thermodynamic” parameter. This parameter cannot simply be the tapping strength since the system can be found in states characterized by the same tapping strength $1/K$ and the same density ρ , that nonetheless evolve in different ways under further tapping with the same strength $1/K$: this is illustrated in Fig. 2b. A natural candidate for an additional thermodynamic parameter is the available line fraction Φ . One can indeed check that the two states described above do correspond to distinct values of Φ .

3. Statistical-mechanical formalism with two thermodynamic parameters

Following the ideas put forward by Edwards and coworkers[9, 10, 11], we consider a statistical-mechanical description of the system in which all possible microstates characterized by a (small) number of fixed macroscopic quantities are assumed to be equiprobable

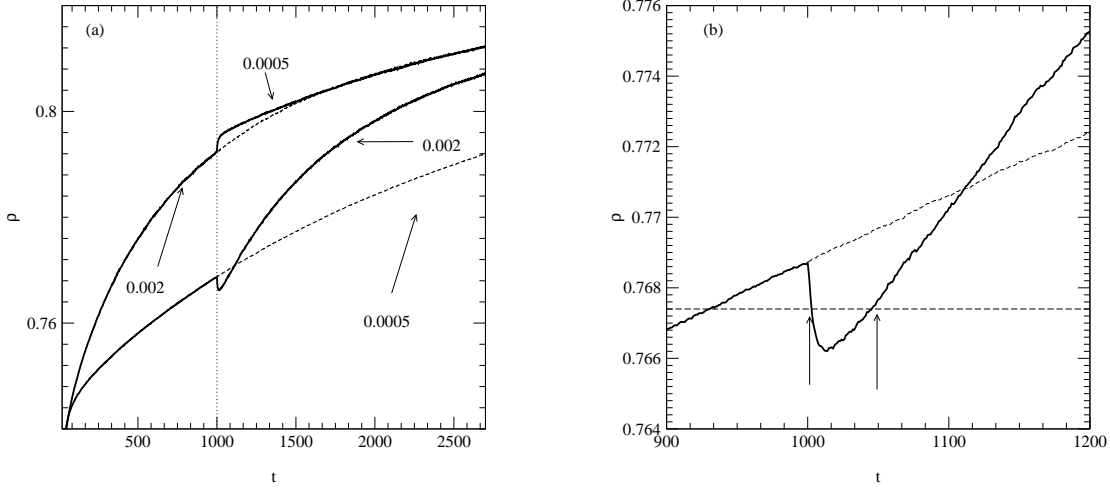


Figure 2. Memory effect: (a) density versus time when the tapping strength is switched from $5.e^{-4}$ to $2.e^{-3}$ (lower full curve) at $t = 1000$ and from $2.e^{-3}$ to $5.e^{-4}$ (upper full curve). The dashed curves correspond to a constant strength, $5.e^{-4}$ (lower curve) and $2.e^{-3}$ (upper curve); (b) Zoom up on the region around $t = 1000$ when one switches from $1/K = 5.e^{-4}$ to $2.e^{-3}$. The arrows denote two points at the same density and same tapping strength $1/K$.

(“flat” or microcanonical distribution). In addition to fixing the density ρ , the parameter originally selected in the compactivity-based description of granular media by Edwards and coworkers, we also constrain the microcanonical ensemble by fixing the available line fraction Φ to account for the above discussion.

Denoting by A the total length available for insertion of a particle center ($A = \Phi L$), the configurational integral with the constraints of fixed A , fixed system size L , and fixed number of particles N is obtained as[35]

$$Z(L, N, A) = \int_0^L \dots \int_0^L \prod_{i=1}^N dh_i \delta \left(L - N - \sum_{i=1}^N h_i \right) \delta \left(A - \sum_{i=1}^N \theta(h_i - 1)(h_i - 1) \right), \quad (4)$$

which can be rewritten as

$$Z(L, N, A) = \int_C dz \int_{C'} dy \exp \left(L \left[z(1 - \rho) + y\Phi + \rho \ln \left(\frac{z + y(1 - \exp(-z))}{z(z + y)} \right) \right] \right) \quad (5)$$

where C and C' denote two closed contours. In the macroscopic limit, $N \rightarrow \infty$, $L \rightarrow \infty$, $A \rightarrow \infty$ with ρ and Φ fixed, one can use a saddle-point method to evaluate the integrals, which leads to

$$Z(L, N, A) \simeq \exp(Ls(\rho, \Phi)) \quad (6)$$

where the entropy density $s(\rho, \Phi)$ is given by

$$s(\rho, \Phi) = (1 - \rho)z + y\Phi + \rho \ln \left(\frac{z + y(1 - \exp(-z))}{z(z + y)} \right), \quad (7)$$

with $z \equiv z(\rho, \Phi)$ and $y \equiv y(\rho, \Phi)$ solutions of the two coupled equations

$$\left(\frac{1 - \rho}{\rho} \right) = \frac{1}{z} + \frac{1}{z + y} - \frac{1 + ye^{-z}}{z + y(1 - e^{-z})}, \quad (8)$$

$$\frac{\Phi}{\rho} = \frac{1}{z + y} - \frac{1 - e^{-z}}{z + y(1 - e^{-z})}. \quad (9)$$

The gap distribution functions can also be derived along the same lines[35], which leads to

$$G_{Ed}(h; \rho) = \begin{cases} \rho \frac{z(z + y)}{z + y(1 - e^{-z})} e^{-zh} & \text{for } h < 1, \\ \rho \frac{z(z + y)}{z + y(1 - e^{-z})} e^{-(zh+y(h-1))} & \text{for } h > 1. \end{cases} \quad (10)$$

It can also be shown that the multi-gap distribution functions satisfy a factorization property, e.g., $G_{Ed}(h, h'; \rho, \Phi) = G_{Ed}(h; \rho, \Phi)G_{Ed}(h'; \rho, \Phi)$. Note that the 1-gap distribution function is a piecewise continuous function that obeys the exact sum rules, Eqs. (2) and (3).

A detailed comparison between the predictions of this statistical-mechanical treatment and simulation data *at the same* ρ and Φ can be found in Ref.[35]. The conclusion is that although not exact, and even missing some qualitative features in the limiting case of a purely irreversible RSA process, the approach provides an overall good description of the data. (It becomes of course exact in the steady state since this latter corresponds to an equilibrium situation.)

4. Approximate description of the compaction kinetics

A quasi-thermodynamic approach is useful because it allows to predict the structure of the system (correlation functions) as well as the fluctuations at any given state point (here assumed to be characterized by ρ and Φ). In the cases where phase transitions occur, it can also provide interesting constraints and relations between the parameters characterizing the phases at the transition or help to determine the limit of stability of the phases in mean-field like treatments. However, one still faces the problem of predicting the state of the system *for a given protocol and a given history*: in the simplest case, for a given time t and a given tapping strength $1/K$.

We thus want to push the Edwards formalism one step further. Predicting the trajectory made by the system in the (ρ, Φ) diagram for a given protocol amounts to determine a system of equations relating ρ and Φ with t and K . Eq. (1) is one such equation. To obtain another equation for the evolution of Φ , we start for the exact kinetic equation for the 1-gap distribution function for $h \geq 1$:

$$\frac{\partial G(h, t)}{\partial t} \Big|_K = -(h-1)G(h, t) + 2 \int_{h+1}^{\infty} dh' G(h', t) - \frac{2G(h, t)}{K} + \frac{1}{K} \int_0^{h-1} dh' G(h', h-1-h', t),$$

(11)

where $G(h, h', t)$ is the 2-gap distribution function that satisfies the “sum rule”

$$\int_0^\infty dh' G(h, h', t) = \rho(t) G(h, t). \quad (12)$$

Note that the approximate 2-gap distribution function $G_{Ed}(h, h')$ satisfies the above sum rule. By multiplying Eq. (11) by $(h - 1)$, integrating over h from 1 to ∞ , and using the sum rules, Eqs. (2), (3) and (12), one obtains an exact equation for the evolution of Φ :

$$\frac{\partial \Phi(t)}{\partial t} \Big|_K = \frac{2}{K} (1 - \rho(t) - \Phi(t)) - \int_1^\infty dh (h-1)^2 G(h, t) + \int_2^\infty dh (h-2)^2 G(h, t). \quad (13)$$

If one now inserts the approximate expression of the 1-gap distribution function, Eq. (10), in the above equation, one gets

$$\frac{\partial \Phi}{\partial t} \Big|_K = \frac{2(1 - \rho(t) - \Phi(t))}{K} - 2\Phi(t) \frac{1 - e^{-(y(t) + z(t))}}{y(t) + z(t)}. \quad (14)$$

Eqs. (1), (8), (9) and (14) form a closed set of equations whose solution for given initial conditions completely characterizes the system and its evolution.

We first test the accuracy of the above approximate kinetic description in two limiting cases for which the exact solution is known: the purely irreversible RSA case ($1/K = 0$) and the approach to the steady state ($t \rightarrow +\infty$) for a given rate K . The steady state corresponds to the solution $z_\infty = \frac{\rho_\infty}{1-\rho_\infty}$, $y_\infty = 0$, where ρ_∞ is the equilibrium density of hard rods at constant activity $1/K$: $\rho_\infty = K\Phi_\infty$ with $\Phi_\infty = (1 - \rho_\infty) \exp\left(\frac{-\rho_\infty}{1-\rho_\infty}\right)$; it is thus the exact result. The approach to the steady state is obtained by linearizing the kinetic equations around the equilibrium solution. One then obtains the following coupled linear differential equations :

$$\frac{\partial y(t)}{\partial t} \Big|_K = -2 \frac{(z_\infty + 1)(e^{-2z_\infty} - 1) + 2(1 + z_\infty^2)e^{-2z_\infty}}{z_\infty(2e^{z_\infty} - z_\infty^2 - 2z_\infty - 2)} y(t) \quad (15)$$

$$\frac{dz(t)}{dt} \Big|_K = -\frac{6e^{z_\infty} - 2z_\infty^2 - 6 - 8z_\infty + (2 + z_\infty^2)z_\infty e^{-z_\infty}}{z_\infty(2e^{z_\infty} - z_\infty^2 - 2z_\infty - 2)} y(t) - \frac{z_\infty + 1}{z_\infty} (z(t) - z_\infty). \quad (16)$$

The associated eigenvalues are all negative and that corresponding to the inverse of relaxation time goes for large K as

$$\tau^{-1} = \Gamma \sim \frac{\ln(K)^2}{3K}. \quad (17)$$

The relaxation time is of the same order of magnitude as that obtained in the simple adiabatic approximation[3] and is much smaller than the exact result (see above). The error comes from the inability of the Edwards approximation to account for the non-exponential behavior of the 1-gap distribution function for $0 \leq h \leq 1$.

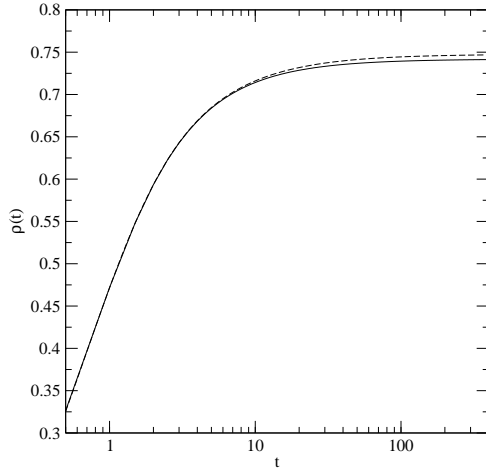


Figure 3. Density versus time for the model without desorption (RSA): the full curve corresponds to the approximation, the dashed curve is the exact result.

On the other hand the approximate kinetic description is very good in the purely irreversible case, $1/K = 0$, (but it still misses some features, as discussed above and in Ref.[35]). Then Eqs. (1) and (14) simplify to

$$\frac{\partial \rho}{\partial t} = \Phi(t) \quad (18)$$

$$\frac{\partial \Phi}{\partial t} = -2\Phi(t) \frac{1 - e^{-(y(t) + z(t))}}{y(t) + z(t)}, \quad (19)$$

where y and z are related to ρ and Φ by Eqs. (8) and (9). It is easy to show that at long times $z(t)$ goes to a finite limit whereas $y(t)$ goes to ∞ as t . As a result the kinetics approaches a non-trivial jamming limit with an algebraic $1/t$ behavior. The numerical solution of the approximate equation shows that the saturation density at the jamming limit $\rho_{JL}^{Ed} \simeq 0.7422$ is very close to the exact value, $\rho_{JL} = 0.74759\dots$. The overall agreement with the exact density evolution is very good, as shown in Fig. 3.

5. Memory and Kovacs Effects

Finally, we apply the approximate kinetic equations to the description of memory effects. By introducing Φ as the second state variable, one expects to obtain a response to a sudden change of the tapping strength that captures these memory effects. This is indeed illustrated in Fig. 4a that shows how the density evolves when K is changed at $t = 60$ from $K = 500$ to $K = 5000$ and from $K = 500$ to $K = 200$. At longer times, note that the density curve corresponding to the change from $K = 500$ to $K = 200$ crosses two times

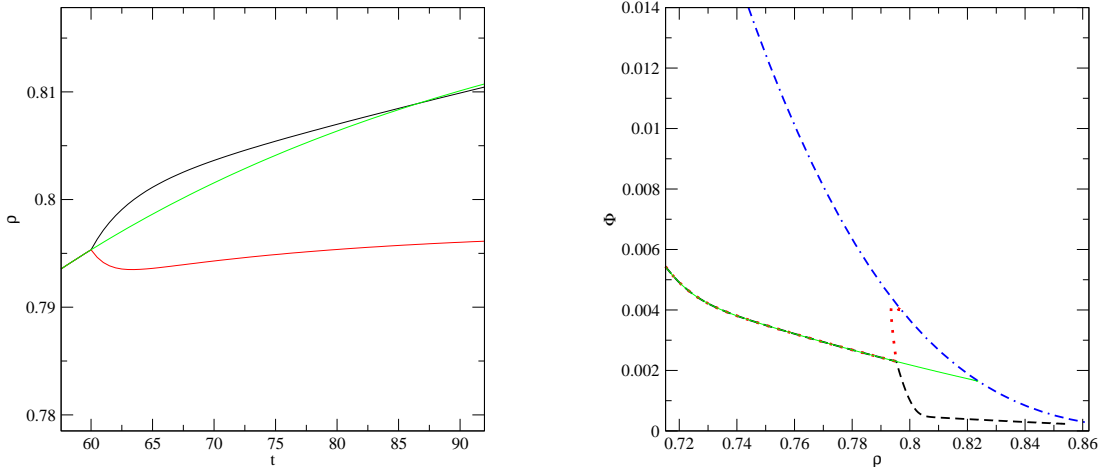


Figure 4. (a) Approximate time evolution of the density for three cases: $K = 500$ (full curve), $K = 500$ from $t = 0$ to $t = 60$ and $K = 200$ for $t > 60$ (dotted curve) and $K = 500$ from $t = 0$ to $t = 60$ and $K = 5000$ for $t > 60$ (dashed curve). (b) Parametric plot of insertion probability Φ versus density for the three above cases. For completeness, the equilibrium insertion probability is added (dash-dot curve).

the density curve calculated when $K = 200$ is kept constant along the process. This is the signature of a Kovacs-like effect which is more clearly displayed in the parametric plot of Fig. 4b: instead of going monotonically to the final value, the density decreases first and passes by a minimum after increasing again. This non-monotonic behavior of the density (or the volume) is precisely the Kovacs effect. The same phenomenon is illustrated for different values of the tapping strength in Figs 5a and b: K is switched from 5000 to 500 or from 5000 to 2000 after a time $t = 250$. In the former case, the density reached at $t = 250$ when K is changed is higher than the final (equilibrium) density reached at $K = 500$; nonetheless, the density starts by first decreasing to a value less than the final density until it reaches a minimum and finally increases again. On the other hand, no minimum is observed in the latter case.

The Kovacs effect is traditionally represented as a “hump” in the volume as a function of time[27, 30, 31]. The position and the height of the hump vary with the waiting time, i.e., the time spent at the initial tapping strength (recall that the process of compaction is always out of equilibrium), and with the amplitude of the shift in the tapping strength (or in other glassy systems, the shift in temperature). The same behavior is found here. It is illustrated in Fig. 6 where we show the evolution of the inverse density for different protocols to reach the equilibrium steady state at $K = 500$: in the upper curve, K is switched from 5000 to 500 at $t_w = 240$, in the intermediate curve K is switched from 2000 to 500 at $t_w = 169$ and in the lower curve $K = 1000$ at $t_w = 139$. The waiting time t_w is

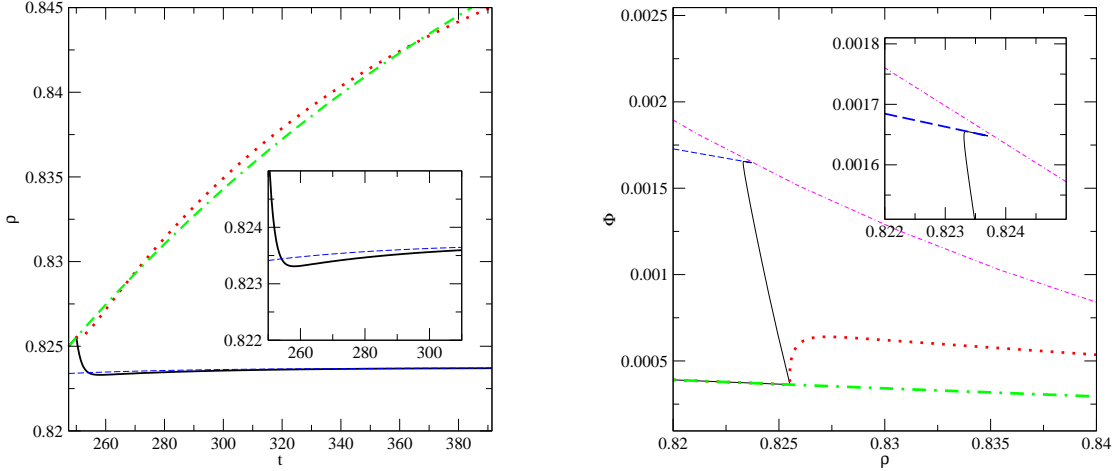


Figure 5. (a) Approximate time evolution of the density for three cases: $K = 500$ (lower curve), $K = 5000$ (dot-dashed curve), $K = 5000$ from $t = 0$ to $t = 250$ and $K = 500$ for $t > 250$ (full curve) and $K = 5000$ from $t = 0$ to $t = 250$ and $K = 2000$ for $t > 60$ (dotted curve). (b) Parametric plot of the insertion probability Φ versus density for the four above cases: For completeness, the equilibrium insertion probability is added (dashed curve).

chosen that the density reached at that time is equal to final density, $\rho_{eq}(K = 500)$. One observes that the height of the hump increases as the amplitude of the shift increases. The Kovacs effect, also observed in the simulation data (not shown here), results from competing trends that are qualitatively well accounted for by the present description in terms of two thermodynamic parameters. Including Φ in the statistical-mechanical treatment is crucial for reproducing such behavior.

6. Conclusion

We have applied a two-parameter statistical-mechanical formalism inspired by the work of Edwards and coworkers to describe the compaction kinetics of the parking-lot model. The approximation gives a fair description of the kinetics, although it underestimates the relaxation time characteristic of the final approach to equilibrium. Inclusion of a second thermodynamic parameter allows one to qualitatively reproduce experimentally observed memory effects in granular compaction and to predict a Kovacs effect similar to what is observed in many glassy systems.

REFERENCES

[1] J. B. Knight, C. G. Fandrich, C. N. Lau, H. M. Jaeger, and S. R. Nagel, Phys. Rev. E **51**, 3957 (1995).

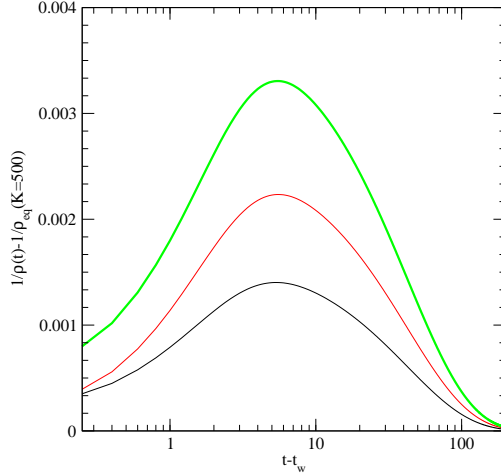


Figure 6. Kovacs effect in the approximate description of the parking-lot model : $1/\rho(t) - 1/\rho_{eq}(K = 500)$ versus $t - t_w$. In the upper curve K is switched from $K = 5000$ to $K = 500$ at $t_w = 240$, in the intermediate curve K is switched from $K = 2000$ to $K = 500$ at $t_w = 169$, and in the lower curve, K is switched from 1000 to 500 at $t_w = 139$.

- [2] E. R. Nowak, J. B. Knight, E. Ben-Naim, H. M. Jaeger, and S. R. Nagel, Phys. Rev. E **57**, 1971 (1998).
- [3] E. Ben-Naim, J. B. Knight, E. R. Nowak, H. M. Jaeger, and S. R. Nagel, Physica D **123**, 380 (1998).
- [4] C. Josserand, A. Tkachenko, D. Mueth, and H. Jaeger, Phys. Rev. Lett. **85**, 3632 (2000).
- [5] P. Philippe and D. Bideau, Europhys. Lett. **60**, 677 (2002).
- [6] J.-P. Bouchaud, in *Slow Relaxations and Nonequilibrium Dynamics in Condensed Matter*, Vol. 77 of *Les Houches-Ecole d'Ete de Physique Theorique*, edited by J. L. Barrat, M. Feigelman, J. Kurchan, and J. Dalibard (Springer-Verlag, Berlin, 2003).
- [7] J.-P. Bouchaud, L. Cugliandolo, J. Kurchan, and M. Mezard, in *Spin Glasses and Random Fields* (World Scientific, Singapore, 1998), p. 161.
- [8] A. Liu and S. Nagel, *Jamming and Rheology: constrained dynamics* (Taylor and Francis, London, 2001).
- [9] A. Mehta and S. Edwards, Physica A **157**, 1091 (1989).
- [10] S. Edwards and R. Oakeshott, Physica A **157**, 1080 (1989).
- [11] S. Edwards, in *Granular Matter: An Interdisciplinary Approach*, edited by A. Mehta (Springer-Verlag, New York, 1994).
- [12] S. Edwards and D. Grinev, Phys. Rev. E **58**, 4758 (1999).
- [13] A. Barrat, J. Kurchan, V. Loreto, and M. Sellitto, Phys. Rev. Lett. **85**, 503 (2000).
- [14] A. Barrat, V. Colizza, and V. Loreto, Phys. Rev. Lett. **66**, 011310 (2002).

- [15] D. Dean and A. Lefèvre, Phys. Rev. Lett. **90**, 198301 (2003).
- [16] A. Lefèvre, J. Phys. A.: Math. Gen. **35**, 9037 (2002).
- [17] J. Berg, S. Franz, and M. Sellitto, Eur. Phys. J. B **26**, 349 (2002).
- [18] A. Coniglio, A. Fierro, and M. Nicodemi, cond-mat/0305175 (2003).
- [19] A. Prados and J. Brey, Phys. Rev. E **66**, 041308 (2002).
- [20] X. Jin, G. Tarjus, and J. Talbot, J. Phys. A.: Math. Gen. **27**, L195 (1994).
- [21] P. L. Krapivsky and E. Ben-Naim, J. Chem. Phys. **100**, 6778 (1994).
- [22] A. Kolan, E. Nowak, and A. Tkachenko, Phys. Rev. E **59**, 3094 (1999).
- [23] J. Talbot, G. Tarjus, and P. Viot, J. Phys. A.: Math. Gen. **32**, 2997 (1999).
- [24] J. Talbot, G. Tarjus, and P. Viot, Eur. Phys. J. E **5**, 445 (2001).
- [25] J. Talbot, G. Tarjus, and P. Viot, Phys. Rev. E **61**, 5429 (2000).
- [26] J. Talbot, G. Tarjus, and P. Viot, Fractals **11**, 185 (2003).
- [27] A. Kovacs, Fortschr. Hochpolym. Forsch. **3**, 394 (1963).
- [28] L. Struik, *Physical Aging in Amorphous Polymers and Other Materials* (Elsevier, New York, 1978).
- [29] L. Berthier and J.-P. Bouchaud, Phys. Rev. B **66**, 054404 (2002).
- [30] S. Mossa and F. Sciortino, cond-mat/0305526 (2003).
- [31] E. Bertin, J.-P. Bouchaud, J.-M. Drouffe, and C. Godrèche, cond-mat/0306089 (2003).
- [32] A. Buhot, cond-mat/0310311 (2003).
- [33] J. Evans, Rev. Mod. Phys. **65**, 1281 (1993).
- [34] J. Talbot, G. Tarjus, P. V. Tassel, and P. Viot, Colloids and Surf. A: **165**, 287 (2000).
- [35] G. Tarjus and P. Viot, cond-mat/0307267 (2003).